Phase Separation and Ordering in Group-III Nitride Alloys

L. K. Teles, M. Marques, L. M. R. Scolfaro, J. R. Leite,
Instituto de Física, Universidade de São Paulo, CP 66318, 05315-970 São Paulo, SP, Brazil

and L. G. Ferreira
Instituto de Física Gleb Wataghin, Universidade Estadual de Campinas, CP 6165, 13083-970 Campinas, SP, Brazil

Received on 9 March, 2003

The electronic, structural, and thermodynamic properties of cubic ($zinc\ blende$) group-III nitride ternary $In_xGa_{1-x}N$ and quaternary $Al_xIn_yGa_{1-x-y}N$ alloys are investigated by combining first-principles total energy calculations and cluster expansion methods. External biaxial strain on the alloys are taken into account in the calculations. While alloy fluctuations and strain effects play a minor role in the physical properties of $AlGaN$, due to the small lattice-mismatch, in the $InGaN$ alloys we found a remarkable influence of strain on the phase separation. The effect of biaxial strain on the formation of ordered phases has been also investigated, and the results are used to clarify the origin of the light emission process in $In_xGa_{1-x}N$ based optoelectronic devices. The dependence of the lattice constant and energy bandgap in quaternary $Al_xIn_yGa_{1-x-y}N$ alloys was obtained as function of the compositions x and y.
PACS: 61.66.Dk, 64.75.+g, 71.20.Nr

1 Introduction

In the last years great progress has been made on the development of optical and electronic devices based on group-III nitride compounds InN, GaN, AlN, and their alloys. Laser diodes (LDs) and light-emitting diodes (LEDs) operating in the short wavelength visible and ultraviolet (UV) spectral regions have been successfully fabricated [1, 2]. An usual feature of these device structures is the utilization of ternary ($In_xGa_{1-x}N$, $Al_xGa_{1-x}N$, or $In_xAl_{1-x}N$) and quaternary ($Al_xGa_yIn_{1-x-y}N$) alloys. The alloying between III-nitride compounds allows a wide-range band gap engineering, which covers from infrared, $\approx 0.7 - 0.9$ eV (InN) till deep UV, 6.3 eV (AlN) [3, 4]. Some examples are: i) high-frequency and high-temperature electronic devices, such as field-effect transistors using $AlGaN/GaN$ quantum wells (QWs) [5]; ii) the recently produced UV- LEDs and LDs comprising quaternary $AlGaInN/AlGaInN$ multiple QWs [6, 7, 8, 9]; iii) the light emitters, which usually comprise $InGaN$ as the active layer. Although the devices are currently produced, the mechanism of light emission for example in these $InGaN$ layers is still subject of discussion. It has been argued that self-organized nanometer scale In-rich quantum dots (QDs), originated from In-segregation taking place in the $In_xGa_{1-x}N$ alloys, are the source of a radiative recombination channel emitting in the blue-green region of the spectrum [10, 11, 12, 13]. It was also shown that the effect of biaxial strain induced by a pseudomorphic growth process in $InGaN$ leads to phase separation suppression effects [14]. In addition to the phase separation process, chemical ordering on the group-III sublattice of $InGaN$ has been reported [15, 16]. Although these ordered phases have been already experimentally observed, there is no systematic theoretical study of the possible existence of bulk ordered structures and the stability of them, as well as, its relation with biaxial strain.

As mentioned, the interest in the quaternary $AlGaInN$ alloys has recently been increased due to their importance to fabricate efficient UV LEDs and LDs. The possibility of alloying using In, besides of Al, makes the $Al_xGa_yIn_{1-x-y}N$ alloy more flexible, e.g. allowing for the production of lattice-matched $AlGaInN$ to GaN layers. The lack of strain in such structures is responsible for much more efficient luminescence arising from the quaternary alloy layer region [17]. Despite the already existent experimental work on quaternary $AlGaInN$ alloys, very few attempts have been conducted on theoretical predictions of their physical properties [18].

In this work, we present a theoretical study of electronic, structural, and thermodynamic properties of group-III nitride ternary $In_xGa_{1-x}N$ and quaternary $In_xAl_yGa_{1-x-y}N$ alloys. The study is performed by carrying out first-principles total energy calculations, in the framework of the density functional theory and the local density approximation, in combination with cluster expansion methods. The energetics and thermodynamic properties of $In_xGa_{1-x}N$ are analyzed in detail, with emphasis on the role played by the biaxial strain and the formation of ordered phases. In case of quaternary $Al_xGa_yIn_{1-x-y}N$ alloys, we show the results obtained for the lattice parameter and band gap energy as functions of the alloy compositions x and y.

2 Calculation methods

In order to access the physical properties of the alloys, we used first-principles total energy calculations together with a cluster expansion method (CEM), within two approaches, the generalized quasi-chemical approximation (GQCA) and through Monte Carlo (MC) simulations. The calculated properties shown here for unstrained $InGaN$ alloys were obtained through the GQCA [19, 20]. For the *strained* $InGaN$ alloy pseudomorphically grown on a rigid *zinc blende* GaN (001) buffer layer, an Ising expansion for the alloy energy and the MC approach have been adopted [21, 22, 23, 24]. The GQCA method used by us to study the ternary nitrides was generalized to treat the quaternary $AlInGaN$ alloys [19, 20].

Total energy and electronic structure calculations of each basic configuration required by the CEM are carried out by using a pseudopotential method (*Vienna Ab-initio Simulation Package* - VASP) within the framework of the density functional theory and the local density approximation [25]. Two structures are assumed for $InGaN$, zinc blende, to describe the fully relaxed (*unstrained*) alloy and tetragonal, to simulate the biaxially strained alloy. Eight- and sixteen-atom supercells were adopted for the calculations of the ternary and quaternary alloys, respectively. Details of the calculation methods may be found elsewhere [19, 20, 26].

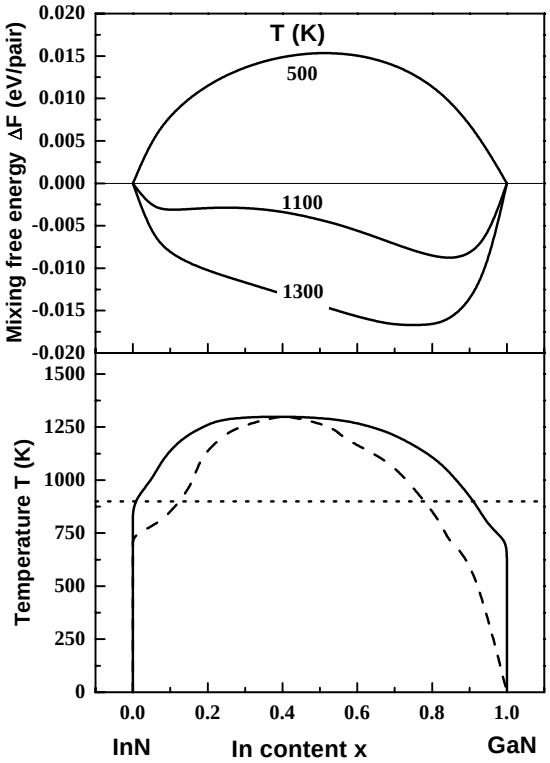

Figure 1. Calculated mixing free energy, ΔF, for three different temperatures (upper), and phase diagram, T versus In content x (lower), for the ternary *unstrained* $In_xGa_{1-x}N$ alloy. In the lower part, binodal (spinodal) curve corresponds to the solid (dashed) line, and the horizontal dotted line marks a typical growth temperature, T$\approx$ 900 K.

3 Results and Discussion

A. $In_xGa_{1-x}N$ ternary alloys

Figure 1 shows the calculated alloy mixing free energy, ΔF, and corresponding phase diagram, $T \times x$, for the *unstrained* ternary $In_xGa_{1-x}N$ alloy. The phase diagram (shown in the lower part of Fig. 1) is easily accessed from the curves of ΔF (shown in the upper part of Fig. 1) [19, 20]. For typical growth temperatures, $T \approx 900$ K, there is a large miscibility gap, therefore indicating that fully relaxed $InGaN$ alloys present phase separation effects, or spinodal decomposition, with an In-rich phase of $x \approx 0.8$. Very similar features are obtained when MC simulations are used. This result is in very good agreement with x-ray diffraction and Raman spectroscopy measurements performed on cubic $InGaN$ thick layers grown on GaAs(001) substrates by molecular beam epitaxy [27].

Contrary to the case of thick $InGaN$ layer samples, in which the $InGaN$ alloy is unstrained, there are evidences that the presence of a biaxial strain may drive the formation of ordering domains in III-V alloys [28]. The energetics and thermodynamic stability of ordered phases in $InGaN$ were studied by combining the *ab initio* total energy calculations with the CEM and MC simulations. The generalized Ising Hamiltonian, or the energy expansion in terms of multisite interaction energies allows us to search for the ground state of $In_xGa_{1-x}N$, by comparing the energies of different structures at the same alloy composition x. The results can be summarized as follows: i) The biaxial strain induced by the GaN buffer suppresses the tendency of the alloy to phase separate and acts as the driving force to form ordered structures at certain stoichiometric compositions [14]. There are several ordered structures with energies close to the minimum, which leads to the conclusion that a mixture of ordered phases or domains of ordered phases with different In content may arise depending on the growth conditions. ii) The lowest energies for the strained alloys occur at the neighborhood of the [3,3] ordered superlattice (corresponding to alternate planes of In and Ga, in number of three of each kind) implying that the composition $x \cong 0.5$ is the most favorable ordered phase, i.e., $In_{0.5}Ga_{0.5}N$.

Ordering in the alloy takes place only below a critical temperature, the stability limit temperature, T_c. Temperatures higher than T_c drive the alloy to a disordered phase. Fig. 2 shows schematically the ordered/disordered transition for the [3,3] $In_{0.5}Ga_{0.5}N$ superlattices, arising from our MC simulations ($T_c = 1487$ K).

Recently, high-resolution x-ray diffraction (HRXRD) and photoluminescence (PL) experiments were combined

to show the presence of strained nanometer scale In-rich phases (QDs) in cubic $GaN/In_xGa_{1-x}N/GaN$ double heterostructures (DHs) with $InGaN$ layer thickness of 30Å [13]. Fig. 3 shows the distribution of the scattered x-ray intensities in reciprocal space (reciprocal space map) of the asymmetric $(\bar{1}\bar{1}3)$ Bragg reflexes of one of the $GaN/InGaN/GaN$ DHs with alloy layer composition $x = 0.33$. A strained In-rich phase with $x = 0.54$ is clearly observed in the map. Since the [3,3] structure is favored in the theoretical calculations, we may conclude that the observed In-rich phase is an ordered structure. Transmission electron microscopy (TEM) experiments on the DHs are underway to confirm this prediction.

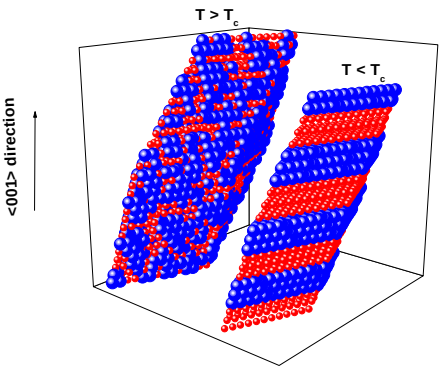

Figure 2. MC simulations showing disordered ($T > T_c$) and the [3,3] ordered ($T < T_c$) structures for the $InGaN$ alloy. Only the Ga and In atoms are schematically shown. $T_c = 1487$ K.

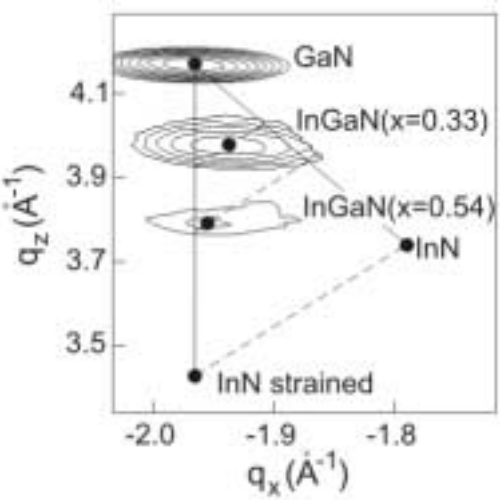

Fig. 3. Reciprocal space maps of the asymmetric $(\bar{1}\bar{1}3)$ Bragg reflexes of a cubic $GaN/In_xGa_{1-x}N/GaN$ DH with alloy layer composition $x = 0.33$. The In content in the separated phase is $x = 0.54$. The position of the maximum intensity of the GaN and $InGaN$ Bragg reflexes of strained and relaxed $InGaN$ layers of varying In content are indicated by full lines. The position of the Bragg reflexes of a partially relaxed $InGaN$ layer of a given composition is shown by dashed lines.

B. $Al_xGa_yIn_{1-x-y}N$ quaternary alloy

We now discuss the results for the quaternary $AlGaInN$ alloy. Fig. 4 shows the calculated lattice constant $a(x, y)$ for $Al_xGa_yIn_{1-x-y}N$. We observe, as in the case of other ternary alloys, a linear behavior of a with the composition. If we consider any composition of one of the alloy components as being fixed, the Vegard's law is fulfilled , in other words $a(x, y) = xa_{AlN} + ya_{GaN} + (1 - x - y)a_{InN}$, with a_{XN} being the lattice constant of the binary alloy XN, $X = Al, Ga, In$. Excellent agreement is observed between theory and experimental data obtained from XRD measurements (squares and triangles in the figure) [29, 30].

In Fig. 5 the calculated direct $(\Gamma - \Gamma)$ energy band gap for $Al_xGa_yIn_{1-x-y}N$ is depicted as a function of Al and Ga contents, x and y. The available experimental data as obtained from PL measurements [30] are also shown for comparison. Good agreement is seen between the theoretical and experimental values. The energy band gap of the quaternary alloy can be well described by an analytical surface equation, which may be useful in future investigations.

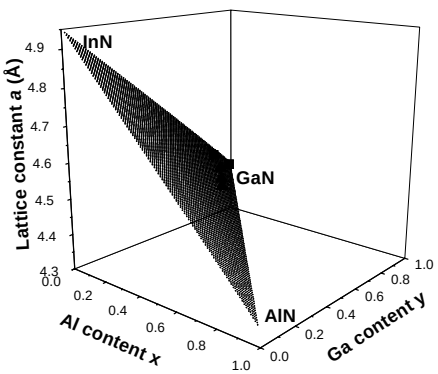

Figure 4. Calculated lattice constant $a(x, y)$ for the quaternary $Al_xGa_yIn_{1-x-y}N$ alloys versus the compositions x and y. Experimental results as extracted from x-ray diffraction measurements, Ref. [29, 30] (solid-triangles and squares).

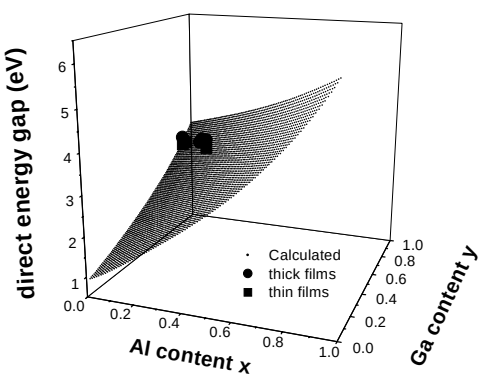

Figure 5. Calculated direct energy bandgap for the quaternary $Al_xGa_yIn_{1-x-y}N$ alloys versus the compositions x and y. Experimental results as extracted from Ref. [30] are shown by solid-circles and squares, corresponding to photoluminescence measurements on thick and thin films, respectively.

4 Conclusion

By using *ab initio* total energy calculations and cluster expansion methods we show that: i) fully relaxed $In_xGa_{1-x}N$ layers undergo phase separation, and ii) biaxial strain induced by thick GaN (001) buffers drives the alloy to separate into ordered phases. Both effects, phase separation and ordering, give rise to self-organized nanometer-scale quantum dots in the $In_xGa_{1-x}N$ layers. The fact that the ordered structure with lowest energy is a superlattice with a period which comprises 3 planes of Ga and 3 planes of In, leads to the conclusion that the strained alloy ground state has a composition $x = 0.5$. We suggest that this finding explains recent TEM and XRD experiments which revealed the presence of ordered $In_{0.5}Ga_{0.5}N$ phase in the hexagonal $In_xGa_{1-x}N$ alloy [15, 16]. Besides, it also explains the presence of In-rich phase with composition of about 0.5 detected from recent XRD experiments performed on cubic $GaN/In_xGa_{1-x}N/GaN$ double heterostructures [13]. Monte Carlo simulations with Metropolis algorithm allowed us to calculate the critical temperature (T_c) for the ordered/disordered transition taking place in the strained alloy. For the ordered structure with lowest energy ($In_{0.5}Ga_{0.5}N$), the value $T_c = 1487$ K was found. This value is above the usual growth temperatures of the $In_xGa_{1-x}N$ layers, as expected. The results presented here concerned to the formation of quantum dots in $InGaN$ layers are important to establish the origin of the luminescence in the nitride-based LDs and LEDs, and to extend the operation of these devices to shorter wavelengths.

The understanding of the electronic, structural and thermodynamic properties of quaternary $Al_xGa_yIn_{1-x-y}N$ alloys is at the beginning. By using the generalized quasi-chemical approximation we calculated the lattice parameter $a(x, y)$ and energy band gap $E_g(x, y)$ of these alloys. While $a(x, y)$ fulfils a Vegard's-like planar law, $E_g(x, y)$ deviates from a planar behavior, displaying a two-dimensional gap bowing in the x, y-plane. The results presented here are very important for tailoring electronic and optoelectronic devices based on $Al_xGa_yIn_{1-x-y}N$ alloys.

Acknowledgments

We acknowledge K. Lischka, D. J. As, D. Schikora, F. Bechstedt, and J. Furthmüller for the fruitful collaboration. This work was supported by FAPESP, CNPq, and CAPES, Brazilian funding agencies.

Note Added in Proof: "An extensive Cluster Expansion revealed that the ground state of the $InGaN$ alloy is a [2,2] (not [3,3]) superlattice in the direction (012) (not (001)) and that the critical temperature for ordering is around 1000 K (not 1400 K)".

References

[1] S. Nakamura, Semic. Sci. Technol. **14**, R27 (1999).

[2] P. Kung and M. Razegui, Opto-electronics review **8**, 201 (2000).

[3] O. Madelung, *Data in Science and Technology: Semiconductors*, Springer-Verlag, Berlin (1991).

[4] V. Yu. Davydov, A. A. Klochikhin, R. P. Seisyan, V. V. Emtsev, S. V. Ivanov, F. Bechstedt, J. Furthmüller, H. Harima, A. V. Mudryi, J. Aderhold, O. Semchinova, and J. Graul, phys. stat. sol. (b)**229**, R1 (2002).

[5] M.A. Khan, J.N. Kuznia, D.T. Olson, W.J. Schaff, J.W. Burm, and M. Shur, Appl. Phys. Lett. **65**, 1121 (1995).

[6] J. Li, B. Nam, K. H. Kim, J. Y. Lin, and H. X. Jiang, Appl. Phys. Lett. **78**, 61 (2001).

[7] V. Adivarahan, A. Chitnis, J. P. Zhang, M. Shatalov, J. W. Yang, G. Simin, M. Asif Khan, R. Gaska, and M. S. Shur, Appl. Phys. Lett. **79**, 4240 (2001).

[8] A. Yasan, R. McClintock, K. Mayes, S. R. Darvish, P. Kung, and M. Razegui, Appl. Phys. Lett. **81**, 801 (2002).

[9] S. Nagahama, T. Yanamoto, M. Sano, and T. Mukai, Jpn. J. Appl. Phys. **40**, L788 (2001).

[10] V. Lemos, E. Silveira, J. R. Leite, A. Tabata, R. Trentin, L. M. R. Scolfaro, T. Frey, D. J. As, D. Schikora, and K. Lischka, Phys. Rev. Lett. **84**, 3666 (2000).

[11] S. Chichibu, T. Azuhata, T. Sota, and S. Nakamura, Appl. Phys. Lett. **69**, 4188 (1996); **70**, 2822 (1997).

[12] K. P. O'Donnell, R. W. Martin, and P. G. Middleton, Phys. Rev. Lett. **82**, 237 (1999).

[13] O. Husberg, A. Khartchenko, D. J. As, H. Vogelsang, T. Frey, D. Schikora, K. Lischka, O. C. Noriega, A. Tabata, and J. R. Leite, Appl. Phys. Lett. **79**, 1243 (2001).

[14] A. Tabata, L. K. Teles, L. M. R. Scolfaro, J. R. Leite, A. Kharchenko, T. Frey, D. J. As, D. Schikora, K. Lischka, J. Furthmüller, and F. Bechstedt, Appl. Phys. Lett. **80**, 769 (2002).

[15] M. K. Behbehani, E. L. Piner, S. X. Liu, N. A. El-Masry, and S. M. Bedair, Appl. Phys. Lett. **75**, 2202 (1999).

[16] P. Ruterana, G. Nouet, W. V. der Stricht, I. Moerman, and L. Considine, Appl. Phys. Lett. **72**, 1742 (1998).

[17] H. Hirayama, A. Kinoshita, T. Yamabi, Y. Enomoto, A. Hirata, T. Araki, Y. Nanishi, and Y. Aoyagi, Appl. Phys. Lett. **80**, 207 (2002).

[18] T. Takayama, M. Yuri, K. Itoh, T. Baba, and J.S. Harris Jr, J. Cryst. Growth **222**, 29 (2001).

[19] L. K. Teles, J. Furthmüller, L. M. R. Scolfaro, J. R. Leite, and F. Bechstedt, Phys. Rev. **B 62**, 2475 (2000); **B 63**, 085204-1 (2001).

[20] L. K. Teles, L. M. R. Scolfaro, J. Furthmüller, J. R. Leite, and F. Bechstedt, J. Appl. Phys. **92**, 7109 (2002).

[21] L. G. Ferreira, S. -H. Wei, and A. Zunger, Int. J. Supercomp. Appl. **5**, 34 (1991).

[22] S. -H. Wei, L. G. Ferreira, and A. Zunger, Phys. Rev. B **45**, 2533 (1992).

[23] Z. W. Lu, S. -H. Wei, A. Zunger, S. Frota-Pessoa, and L. G. Ferreira, Phys. Rev. B **44**, 512 (1991).

[24] N. Metropolis, A. W. Rosenbluth, M. N. Rosenbluth, A. H. Teller, and E. Teller, J. Chem. Phys. **21**, 1087 (1953).

[25] G. Kresse and J. Furthmüller, Comput. Mat. Sci. **6**, 15 (1996); Phys. Rev. B**54**, 11169 (1996).

[26] L. K. Teles, L. G. Ferreira, L. M. R. Scolfaro, and J. R. Leite, Phys. Rev. B - in press.

[27] E. Silveira, A. Tabata, J. R. Leite, R. Trentin, V. Lemos, T. Frey, D. J. As, D. Schikora, and K. Lischka, Appl. Phys. Lett. **75**, 3602 (1999).

[28] A. Zunger, *Handbook of Crystal Growth* vol.3, 998 (D. T. J. Hurle, Elsevier, Amsterdam, 1994).

[29] F. G. McIntosh, K. S. Boutros, J. C. Roberts, S. M. Bedair, E. L. Piner, and N. A. El-Masry, Appl. Phys. Lett. **68**, 40 (1996).

[30] M. E. Aumer, S. F. LeBoeuf, F. G. McIntosh, and S. M. Bedair, Appl. Phys. Lett. **75**, 3315 (1999).